

PlaTe: Visually-Grounded Planning with Transformers in Procedural Tasks

Jiankai Sun¹, De-An Huang², Bo Lu³, Yun-Hui Liu⁴, Bolei Zhou⁵, Animesh Garg^{2,6}

Abstract—In this work, we study the problem of how to leverage instructional videos to facilitate the understanding of human decision-making processes, focusing on training a model with the ability to plan a goal-directed procedure from real-world videos. Learning structured and plannable state and action spaces directly from unstructured videos is the key technical challenge of our task. There are two problems: first, the appearance gap between the training and validation datasets could be large for unstructured videos; second, these gaps lead to decision errors that compound over the steps. We address these limitations with **Planning Transformer (PlaTe)**, which has the advantage of circumventing the compounding prediction errors that occur with single-step models during long model-based rollouts. Our method simultaneously learns the latent state and action information of assigned tasks and the representations of the decision-making process from human demonstrations. Experiments conducted on real-world instructional videos show that our method can achieve a better performance in reaching the indicated goal than previous algorithms. We also validated the possibility of applying procedural tasks on a UR-5 platform. Please see pair.toronto.edu/plate-planner for additional details.

Index Terms—Deep Learning for Visual Perception, Task Planning, Embodied Cognitive Science

I. INTRODUCTION

INTELLIGENT reasoning in embodied environments requires that an agent has explicit representations of parts or aspects of its environment to reason about [1]. As a generic reasoning application, action planning and learning are crucial skills for cognitive robotics. Planning, in the traditional AI sense, means deliberating about a course of actions for an agent to take for achieving a given set of goals. The desired plan is a set of actions whose execution transforms the initial situation into the goal situation (goal situations need not be unique). Normally, actions in a plan cannot be executed in arbitrary sequence, but have to obey an ordering, ensuring that all preconditions of each action are valid at the time of its execution. In practice, there are two challenges for planning. First, typically not all information that would be needed is available. Planning is meant for real environments in which many parameters are unknown or unknowable. Second, even if

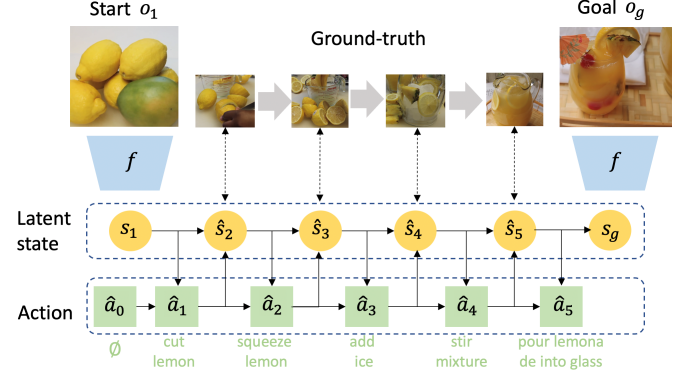


Fig. 1: **PlaTe Overview**. Given a visual observation as start and goal, the encoder $f(\cdot)$ extracts the feature about the planning trajectory. This transformer-based procedure planning model is responsible for learning plannable latent representations \hat{s} and actions \hat{a} .

everything for a complete planning were known, then it would very likely be so computationally intensive that it would run too slowly in the real world. Thus, many planning systems and their underlying planning algorithms accept the restrictive assumptions of information completeness, determinism, instantaneousness, and idleness [1], [2].

Procedure planning in instructional videos [3] (as shown in Figure 1) aims to make goal-conditioned decisions by planning a sequence of high-level actions that can bring the agent from current observation to the goal. Planning in instructional videos is a meaningful task since the ability to perform effective planning is crucial for an instruction-following agent. Although learning from instructional videos is natural to humans, it is challenging for the AI system because it requires understanding human behaviors in the videos, focusing on actions and intentions. How to learn structured and plannable state and action spaces directly from unstructured videos is the key technical challenge of our task.

It is crucial for autonomous agents to plan for complex tasks in everyday settings from visual observations [3]. Although reinforcement learning provides a powerful and general framework for decision making and control, its application in practice is often hindered by the need for extensive feature and reward engineering [4], [5]. Moreover, deep RL algorithms are often sensitive to factors such as reward sparsity and magnitude, making well-performing reward functions particularly difficult to engineer. In many real-world applications, specifying a proper reward function is difficult.

In this paper, we proposed a new framework for procedure planning from visual observations. We address these limitations with a new formulation of procedure planning and

Manuscript received: September 9, 2021; Revised December 7, 2021; Accepted January 10, 2022.

This paper was recommended for publication by Editor Cesar Cadena upon evaluation of the Associate Editor and Reviewers' comments.

¹Stanford University, Stanford, California, United States of America, 94305.

²NVIDIA, Cupertino, CA, United States of America, 95014.

³Robotics and Microsystems Center, School of Mechanical and Electric Engineering, Soochow University, Suzhou, Jiangsu, China.

⁴The Chinese University of Hong Kong, Hong Kong.

⁵University of California, Los Angeles, USA.

⁶University of Toronto & Vector Institute, Canada.

novel algorithms for modeling human behavior through a Transformer-based planning network PlaTe. Our method simultaneously learns the high-level action planning of assigned tasks and the representations of the decision-making process from human demonstrations.

We summarize our contributions as follows:

- We proposed a novel method, Planning Transformer network (PlaTe), for procedure planning in instructional videos task, which enjoys the advantage of long-term planning. We introduce some critical design choices that assist in learning cross-modal correspondence and, more importantly, improve the accuracy of generated planning sequences.
- We integrate Beam Search to PlaTe to prevent it from large search discrepancies, and reduce the performance degradation.
- Experimental results show that our framework outperforms the baselines in the procedure planning task on CrossTask, a real-world dataset. We also validated the possibility of applying procedural tasks on a real UR-5 platform.

II. RELATED WORK

Self-Attention and Transformer. Transformer-based architectures, eschew the use of recurrence in neural networks and instead trust entirely on self-attention mechanisms to draw global dependencies between inputs and outputs. Self-attention [6] is particularly suitable for procedure planning, which can be seen as a sequence modeling task. Compared with Recurrent Neural Networks (RNNs), long short-term memory (LSTM) [7] and gated recurrent neural networks [8], the advantages of self-attention includes avoiding compressing the whole past into a fixed-size hidden state, less total computational complexity per layer, and more parallelizable computations. In this paper, thanks to Transformers' computational efficiency and scalability, we explore the possibility of marrying Transformer-based architecture for procedure planning.

Learning to Plan from Pixels. Another related work is learning dynamics models for model-based RL [9], [10], [11]. Recent works have shown that deep networks can learn to plan directly from pixel observations in domains such as table-top manipulation [12], [13], [14], navigation [15], [16], [17], and locomotion in joint space [18]. Universal Planning Networks (UPN) [13] assumes the action space to be differentiable and uses a gradient descent planner to learn representations from expert demonstrations. Prior work [3] proposes the conjugate dynamics model to expedite the latent space learning, but suffers from compounding error. While they attempt to solve the same problem, however there exist some key methodical differences. Mainly, PlaTe uses a transformer model to plan actions, which results in improved success rate, accuracy, and mIoU. Further, even with a good planner, due to the stochastic nature of predictions, planning is often low quality with a single roll-out. We address this issue with a beam search method. The adversarial training scheme proposed by Bi et al. [19] is a complex, multi-stage pipeline. In contrast, we

implement an end-to-end transformer architecture, simple but efficient.

Learning from Instructional Videos. The interest has dramatically increased in recent years in understanding human behaviors by analyzing instructional videos [20], [21], [22]. Event discovery tasks such as action recognition and temporal action segmentation [23], [24], [25], [26], state understanding [27], video prediction [28] and video summarization / captioning [29], [20] study recognition of human actions in video sequences. The other works [30] perform egocentric action anticipation model the relationships between past, future events, and incomplete observations. Action label prediction [31], [32] addresses the problem of anticipating all activities within a time horizon. However, the correct answer is often not unique due to the large uncertainty in human actions.

III. OUR METHOD: PLATE

A. Problem Setup

We consider a similar setup to [3]: given the start visual observation o_t and a visual goal o_g that indicates the desired outcome for a particular task. During training, we have access to the observation-action pairs $\{(o_{t,g}, a_{t,g})\} \sim \pi_E$ that were collected by an expert attempting to reach the goals. When testing, only the start visual observation o_t and a visual goal o_g are given. Our objective is to plan a sequence of actions $[\hat{a}_t, \dots, \hat{a}_{t+T-1}]$ that can bring the underlying state of o_t to that of o_g . T is the horizon of planning, which means the number of task-level action steps the model is allowed to take. Figure 1 shows a goal-oriented plannable example where the intermediate steps of performing a complex planning task are planned.

Our key insight is that the compounding error can be reduced by jointly learning the state and action representation with Transformer-based architecture. As shown in the overall architecture in Figure 2, the procedure planning problem $p(\hat{a}_{1:T}|o_1, o_g)$ is formulated as maximizing the probability

$$p(\hat{a}_{1:T}|o_1, o_g) = \Pr(\hat{s}_1|o_1)\Pr(\hat{s}_g|o_g)\prod_{t=1}^T \Pr(\hat{a}_t|\hat{s}_t, \hat{a}_{t-1}, \hat{s}_g)\Pr(\hat{s}_{t+1}|\hat{s}_t, \hat{a}_t, \hat{s}_g). \quad (1)$$

In the following sections, we first discuss how to encode the latent semantic representation. Then, we will introduce how to solve the long-term procedure planning task with transformer-based architecture. Lastly, we will discuss how to apply learned representation to solve the procedure planning by integrating Beam Search.

B. Latent Semantic Representation

First, we use the state encoder $\hat{s} = f(o)$ that encodes the visual observation to a latent semantic representation, then added with learnable positional encoding, before they were input into the transformer layers.

The remaining question is: how to learn a planning model $p(\hat{a}_{1:T}, \hat{s}_{1:T}|\hat{s}_1, \hat{s}_g)$ to plan the action sequence and corresponding latent state representation? We assume the underlying process in Figure 1 is a fully observable goal-conditioned Markov

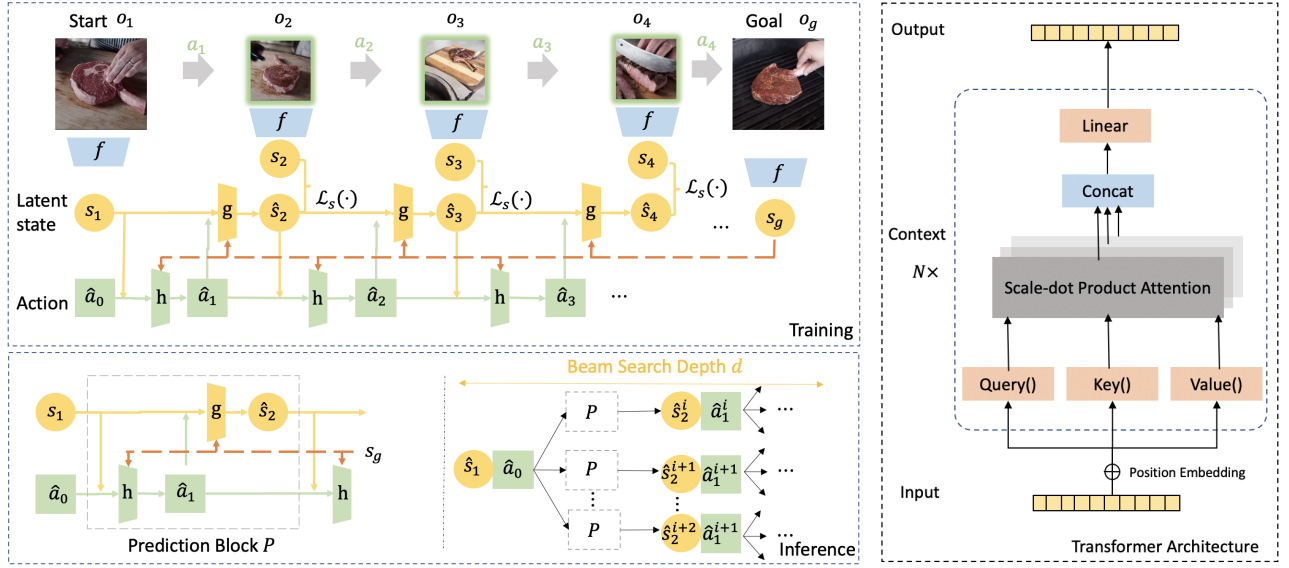


Fig. 2: **PLaTe Framework**. Given the start and goal visual observations, encoder f outputs the latent representations \hat{s} . We set $\hat{a}_0 = 0$. The latent representation and predicted action are inferred using transformer-based action prediction model $h(\cdot)$ and state prediction model $g(\cdot)$. The goal state s_g is an input to both models. During training, the ground-truth action a and state s are given. During inference, we use Beam Search to enhance the trained $h(\cdot), g(\cdot)$. The right part shows the Transformer architecture we used for the planning model. Query(), Key(), and Value() are linear layers.

Decision Process $(\mathcal{S}, \mathcal{A}, \mathcal{T})$, where \mathcal{S} is the state space, \mathcal{A} is the action space, $\mathcal{T}: \mathcal{S} \times \mathcal{A} \rightarrow \mathcal{S}$ is the unknown transition probability distribution. We denote $h(\hat{a}_t | \hat{s}_t, \hat{a}_{t-1}, \hat{s}_g)$ as the *action prediction model* conditioned on the current state, previous action, and goal, $g(\hat{s}_{t+1} | \hat{s}_t, \hat{a}_t, \hat{s}_g)$ as the *state prediction model* conditioned on the previous state, goal, and previous action. They plan the sequence of actions and hidden states from the initial state to the goal state. In this way, we are able to factorize the planning model $p(\hat{a}_{1:T}, \hat{s}_{1:T} | \hat{s}_1, \hat{s}_g)$ as:

$$p(\hat{a}_{1:T}, \hat{s}_{1:T} | \hat{s}_1, \hat{s}_g) = \prod_{t=1}^T h(\hat{a}_t | \hat{s}_t, \hat{a}_{t-1}, \hat{s}_g) g(\hat{s}_{t+1} | \hat{s}_t, \hat{a}_t, \hat{s}_g), \quad (2)$$

where we use the convention that $\hat{s}_0 = 0, \hat{a}_0 = 0$. The data is in the form of tuples (s_t, a_t, s_{t+1}) . We assume to start at s_1 , and reach a goal s_g , in T timesteps. We need to generate an action sequence $a_{1:T}$ of length T , which yields a state trajectory of length $T + 1$.

C. Transition Transformer

We propose a transformer-based network architecture that can learn the action-state correlation and generate planning sequences. The overview of this architecture is shown in Figure 2. Our design choices are explained in detail below.

We introduce two cross-modal transformers: the action transformer $h(\hat{a}_t | \hat{s}_t, \hat{a}_{t-1}, \hat{s}_g)$, which learns the correspondence between previous action feature \hat{a}_{t-1} and state feature \hat{s}_t, \hat{s}_g and generates the action prediction \hat{a}_t ; the state transformer $g(\hat{s}_{t+1} | \hat{s}_t, \hat{a}_t, \hat{s}_g)$, which learns the correspondence between the state feature \hat{s}_t, \hat{s}_g and action feature \hat{a}_t and generates the future state prediction \hat{s}_{t+1} . The model takes as input the whole sequence during training and all past pairs of state-action

during inference, similarly to how transformer-like models usually work.

Specifically, the output of the attention layer, the context vector \mathbf{C} is computed using the query vector \mathbf{Q} and the key \mathbf{K} value \mathbf{V} pair from the input with an upper triangular look-ahead mask \mathbf{M} via

$$\mathbf{C} = \text{Attn}(\mathbf{Q}, \mathbf{K}, \mathbf{V}, \mathbf{M}) = \text{softmax}\left(\frac{\mathbf{Q}\mathbf{K}^T + \mathbf{M}}{\sqrt{D}}\right) \mathbf{V}, \quad (3)$$

where D is the number of channels in the attention layer. The look-ahead-mask \mathbf{M} is a triangular matrix to ensure that the predictions can depend only on the known outputs before.

D. Beam Search in Procedure Planning

Given a transformer planning model P_θ parameterized by θ and an input x , which contains the information of current state, previous action step, and goal state, the problem of procedure planning task consists of finding a action sequence $\hat{\mathbf{a}}$ such that $\hat{\mathbf{a}} = \arg\max_{\mathbf{a} \in \mathcal{A}} P_\theta(\mathbf{a} | x)$, where \mathcal{A} is the set of all sequences. $\mathbf{a} = \{\hat{a}_1, \dots, \hat{a}_T\}$ can be regarded as a sequence of tokens from vocabulary \mathcal{V} , where T is the length of the sequence $\hat{\mathbf{a}}$. Then $P_\theta(\hat{\mathbf{a}} | x)$ can be factored as

$$\begin{aligned} \log P_\theta(\hat{\mathbf{a}} | x) &= \log \prod_{t=1}^T P_\theta(\hat{a}_t | \{\hat{s}_1, \hat{a}_0\}; \dots; \{\hat{s}_t, \hat{a}_{t-1}\}; \hat{s}_g) \\ &= \sum_{t=1}^T \log P_\theta(\hat{a}_t | \{\hat{s}_1, \hat{a}_0\}; \dots; \{\hat{s}_t, \hat{a}_{t-1}\}; \hat{s}_g). \end{aligned} \quad (4)$$

The discrepancy gap is the difference in log-probability between the most likely token and the chosen token [33], [34]. At time step t , the discrepancy gap is

$$\begin{aligned} &\max_{\hat{\mathbf{a}} \in \mathcal{V}} [\log P_\theta(\hat{\mathbf{a}} | \{\hat{s}_1, \hat{a}_0\}; \dots; \{\hat{s}_t, \hat{a}_{t-1}\}; \hat{s}_g) \\ &\quad - \log P_\theta(\hat{a}_t | \{\hat{s}_1, \hat{a}_0\}; \dots; \{\hat{s}_t, \hat{a}_{t-1}\}; \hat{s}_g)]. \end{aligned} \quad (5)$$

Algorithm 1 PlaTe: Planning Inference Phase

Input: sequence \mathbf{x} , Beginning Of Sequence BOS, End Of Sequence EOS, buffer B , buffer size \mathcal{N} , score function $\text{score}(\cdot, \cdot)$, maximum sequence length n_{\max} , maximum beam size k , planning model $p(\hat{s}_t^i, \hat{a}_t^i | \hat{s}_{t-1}^i, \hat{a}_{t-1}^i, \hat{s}_T^i)$

Output: searched sequence $B.\max()$

```

 $B_0 \leftarrow \{< 0, \text{BOS} >\}$ 
for  $t \in \{1, \dots, n_{\max} - 1\}$  do
   $B \leftarrow \emptyset$ 
  for  $< w, (\hat{s}_{t-1}^i, \hat{a}_{t-1}^i, \hat{s}_T^i) > \in B_{t-1}$  do
    if  $\hat{s}_{t-1}^i.\text{last}() = \text{EOS}$  then
       $B.\text{add}(< w, (\hat{s}_{t-1}^i, \hat{a}_{t-1}^i, \hat{s}_T^i) >)$ 
      continue
    end if
     $(\hat{s}_t^i, \hat{a}_t^i) \leftarrow p(\hat{s}_t^i, \hat{a}_t^i | \hat{s}_{t-1}^i, \hat{a}_{t-1}^i, \hat{s}_T^i)$ 
     $w \leftarrow \text{score}(\hat{s}_t^i, \hat{a}_t^i, \hat{s}_T^i)$ 
     $B.\text{add}(< w, (\hat{s}_t^i, \hat{a}_t^i, \hat{s}_T^i) >)$ 
  end for
   $B_t \leftarrow B.\text{top}(k)$ 
end for
return  $B.\max()$ 

```

To avoid long-term procedure planning from significant search discrepancies, we introduce the discrepancy-constrained Beam Search during the *inference phase of procedure planning*. The action log-probability output by action prediction model $h(\cdot)$ is used as the score function. The inference algorithm is shown as Algorithm 1. In this way, we can reduce the performance degradation.

E. Learning

As shown in Figure 2, we have three main components to optimize: state encoder f , action prediction model h , and state prediction model g . We refer to the expert trajectory as $\tau^E = \{(s_t^E, a_t^E)\}$ and predicted trajectory $\tau = \{(\hat{s}_t, \hat{a}_t)\}$ as state-action pairs visited by the current planning model.

We optimize by descending the gradient in Equation 6.

$$\min_{\theta} \sum_{t=1}^T \|\hat{s}_t - s_t^E\|_2 + \text{CE}(\hat{a}_t, a_t^E) \quad (6)$$

where CE is the cross-entropy loss. In training, T -step sequence is output once. In testing, single-step inference is made with Beam Search.

IV. EXPERIMENTS

In our experiments, we aim to answer the following questions: (1) Is PlaTe efficient and scalable to procedure planning tasks? (2) Can PlaTe learn to plan on the interactive environment? To answer Question 1, we evaluate PlaTe on CrossTask, a real-world offline instructional video dataset. We show procedure planning with our algorithm performs better on the CrossTask dataset than previous methods. To answer Question 2, we evaluate our method on a real-world UR-5 robot arm platform.

A. Experimental Setup

Datasets. We first evaluate PlaTe on an instructional video dataset CrossTask [21]. For real-world UR-5 experiments, we collect a *UR-5 Reaching Dataset* which consists of 100 trajectories (2150 first-person-view RGB image and corresponding action pairs) as a training set and evaluate on a real UR-5 platform.

Implementation Details. We compare with the baselines in [3] with the metrics such as success rate, accuracy, and mIoU. We use the Transformer architecture [6] as the transition model with 8 self-attention layers and 8 heads. The transition model is two-headed: one for action prediction the other for state prediction. Let L_s be the hidden dimension for state and L_a be the embedding dimension for action. The state encoder in our model is two fully-connected layers with $[64, L_s]$ units in each layer and Leaky-ReLU as non-linearity function. We encode (o_t, o_g) to be L_s -dim s_t . a_t is encoded (in transformer terminology: "tokenized") to be a L_a -dim embedding and concatenated together with s_t to be provided as input to the transformer. The size of the input of the transformer is $L_s + L_a$ and the size of the output of the transformer is also $L_s + L_a$. s_{t+1} is the first L_s -dim features split from transformer output. a_{t+1} is decoded from the rest of transformer output. In our experiments, $L_s = 32$ and L_a is the total number of possible actions. For CrossTask experiments, $L_a = 105$. One-hot vectors are used for this action classification purpose. During training, all models are optimized by Adam [35] with the starting learning rate of 10^{-4} . We train our model for 200 epochs on a single GTX 1080 Ti GPU.

B. Evaluating Procedure Planning on CrossTask

First, we choose a real-world instructional video dataset CrossTask [21] to conduct our experiments. CrossTask comprises 2,750 videos (212 hours). Each video depicts one of the 18 primary long-horizon tasks. To test the trained agent's generalization capability, for the videos in each task, we randomly divide the videos in each task into 70%/30% splits for training and testing. Each video can be regarded as a sequence of images V_i (where i is the index of frames) that have annotated with a sequence of action labels a_j and each action starts at frame index s_j and ends at frame index e_j . Same as the setup of [3]: we choose frames around the beginning of the captions $V_{s_t - \delta/2 : s_t + \delta/2}$ as o_t , caption description a_t as the semantic meaning of action, and images nearby the end $V_{e_t - \delta/2 : e_t + \delta/2}$ as the next observation o_{t+1} . Here, δ controls the duration of each observation, and we set $\delta = 2$ for all data we have used in our paper. Our state-space \mathcal{S} is the pre-computed features provided in CrossTask: each second of the video is encoded into a 3,200-dimensional feature vector, which is a concatenation of the I3D [36], Resnet-152 [37], and audio VGG features [38]. The action space \mathcal{A} is constructed by enumerating all combinations of predicates and objects, which provides 105 action labels and is shared across all 18 tasks. Our method is suitable for modeling longer trajectories, but we restrict the experiments to horizontal lengths $T = 3 \sim 4$ to maintain a consistent comparison with state-of-the-art methods.

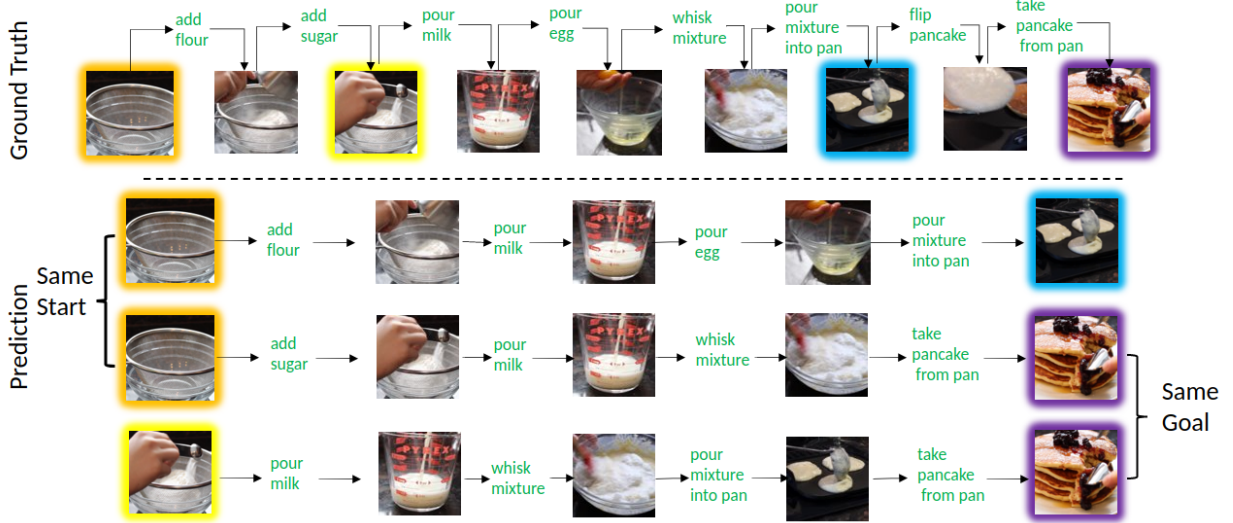


Fig. 3: **Qualitative results of procedure planning on CrossTask.** Qualitative results of procedure planning for *Make Pancakes*. The top row describes the correct action sequence required to “make pancakes”. To examine our method’s robustness, We vary the start and goal observations to evaluate our method. The results show that our approach is robust to perform planning within different stages in the video.

TABLE I: CrossTask Results. Our model outperforms baselines in terms of success rate, accuracy, and mIoU.

Method	Prediction Length $T = 3$			Prediction Length $T = 4$		
	Success Rate (%)	Accuracy (%)	mIoU (%)	Success Rate (%)	Accuracy (%)	mIoU (%)
Random	<0.01	0.94	1.66	<0.01	0.83	1.66
RB [29]	8.05	23.30	32.06	3.95	22.22	36.97
WLTD [18]	1.87	21.64	31.70	0.77	17.92	26.43
UAAA [32]	2.15	20.21	30.87	0.98	19.86	27.09
UPN [13]	2.89	24.39	31.56	1.19	21.59	27.85
DDN [3]	12.18	31.29	47.48	5.97	27.10	48.46
PlaTe (Ours)	16.00	36.17	65.91	14.00	35.29	55.36

Recall that in procedure planning, given the start and goal observations o_1 and o_g , the agent needs to output a valid procedure $\{a_1, \dots, a_T\}$ to reach the specified goal. As illustrated in Table I, as instructional videos’ action space is not continuous, the gradient-based planner of UPN cannot work well. By introducing Beam Search, our PlaTe has a better performance in terms of success rate, accuracy, and mIoU. By designing a model with transformer-based components, we show that our model outperforms all the baseline approaches on real-world videos.

In Figure 3, we visualize some examples of the predicted procedure planning results on CrossTask, where the task is to *Make Pancake*. Our model is able to predict a sequence of actions with correct ordering. Specifically, the most challenging step in *Make Pancake* is the “add flour” and “add sugar” step, where visual differences are not significant, and it can only be inferred from context and sequence relationships.

C. Evaluating Procedure Planning on Real Robot

Previous Procedure Planning research has rarely reported experimental results in real robots. There remains a gap between offline training and real-world applications. To validate the possibility of applying procedural tasks in the real environment, we conduct experiments on “Reaching a block” (cf. Figure 4) using a Universal Robot UR5 system. While this task is easy in simulation, it can be difficult for real robot [39]. Our agent learns to achieve tasks by imitating

TABLE II: Success Rate (%) of UR5.

Method	UR5	
	Prediction Length	
	$T = 3$	$T = 4$
Random	<0.01	<0.01
RB [29]	32	26
RL [3]	50	44
WLTD [18]	42	38
UAAA [32]	44	40
UPN [13]	44	38
DDN [3]	52	46
PlaTe (Ours)	60	52

expert demonstrations. After the RGB-D camera is installed in front of the manipulator, the observation space includes the raw RGB images at the current position and goal position. The action space includes None, Up, Down, Left, Right, Forward, Backward. UR5 Reacher consists of episodes of interactions, where each episode is T time steps long. The fingertip of UR5 Reacher is confined within a 3-dimensional $0.7m \times 0.5m \times 0.4m$ boundary. The robot is also constrained within a joint-angular boundary to avoid self-collision.

In the task of Reaching, the robot is required to start at the current observation and then move to a goal observation. Since the controller of the robot is imperfect, we consider a reach to be successful if the robot reaches within 5cm of the block. The UR5 robotic arm is controlled by human volunteers to reach the target, and thus 100 offline expert demonstration

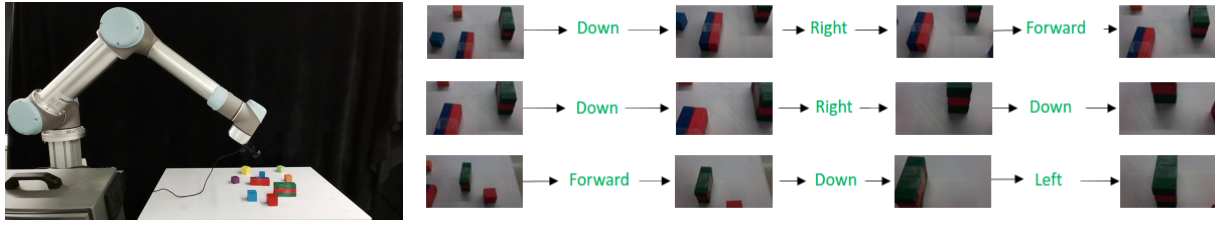


Fig. 4: Qualitative results of procedure planning on UR5.

trajectories are generated. All methods are evaluated on a real UR5 robotic arm for 50 episodes. As shown in Table II, our approach outperforms the other methods. Even though other baselines have succeeded in the offline dataset, real robotic reaching lags far behind human performance and remains unsolved in the field of robot learning.

V. CONCLUSION

To conclude, we propose a cross-modal transformer-based architecture to address the procedure planning problem, which can capture long-term time dependencies. Moreover, We propose to enhance the transformer-based planner with Beam Search. Finally, we evaluate our method on a real-world instructional video dataset. The results indicate that our method can learn a meaningful action sequence for planning and recover the human decision-making process. We also validated the possibility of applying procedural tasks on a real UR-5 platform.

ACKNOWLEDGMENT

Animesh Garg is supported in part by CIFAR AI Chair at the Vector Institute for AI and NSERC Discovery Award.

REFERENCES

- [1] M. Beetz, R. Chatila, J. Hertzberg, and F. Pecora, "Ai reasoning methods for robotics," in *Springer Handbook of Robotics*, 2016.
- [2] J. Sun, H. Sun, T. Han, and B. Zhou, "Neuro-symbolic program search for autonomous driving decision module design," in *Proceedings of the 2020 Conference on Robot Learning*, ser. Proceedings of Machine Learning Research, J. Kober, F. Ramos, and C. Tomlin, Eds., vol. 155. PMLR, 16–18 Nov 2021, pp. 21–30. [Online]. Available: <https://proceedings.mlr.press/v155/sun21a.html>
- [3] C.-Y. Chang, D.-A. Huang, D. Xu, E. Adeli, L. Fei-Fei, and J. C. Niebles, "Procedure planning in instructional videos," in *ECCV*. Springer, 2020, pp. 334–350.
- [4] J. Sun, L. Yu, P. Dong, B. Lu, and B. Zhou, "Adversarial inverse reinforcement learning with self-attention dynamics model," *IEEE Robotics and Automation Letters*, vol. 6, no. 2, pp. 1880–1886, 2021.
- [5] J. Huang, S. Xie, J. Sun, Q. Ma, C. Liu, D. Lin, and B. Zhou, "Learning a decision module by imitating driver's control behaviors," in *Proceedings of the Conference on Robot Learning (CoRL) 2020*.
- [6] A. Vaswani, N. Shazeer, N. Parmar, J. Uszkoreit, L. Jones, A. N. Gomez, L. u. Kaiser, and I. Polosukhin, "Attention is all you need," in *NeurIPS*, vol. 30. Curran Associates, Inc., 2017.
- [7] S. Hochreiter and J. Schmidhuber, "Long short-term memory," *Neural Comput.*, 1997.
- [8] J. Chung, C. Gulcehre, K. Cho, and Y. Bengio, "Empirical evaluation of gated recurrent neural networks on sequence modeling," *arXiv:1412.3555*, 2014.
- [9] D. Hafner, T. Lillicrap, I. Fischer, R. Villegas, D. Ha, H. Lee, and J. Davidson, "Learning latent dynamics for planning from pixels," in *ICML*, 2019.
- [10] K. Fang, Y. Zhu, A. Garg, S. Savarese, and L. Fei-Fei, "Dynamics learning with cascaded variational inference for multi-step manipulation," *arXiv:1910.13395*, 2019.
- [11] B. Amos, S. Stanton, D. Yarats, and A. G. Wilson, "On the model-based stochastic value gradient for continuous reinforcement learning," in *LADC*, 2021, pp. 6–20.
- [12] T. Kurutach, A. Tamar, G. Yang, S. J. Russell, and P. Abbeel, "Learning plannable representations with causal infogan," in *NeurIPS*, vol. 31. Curran Associates, Inc., 2018, pp. 8733–8744.
- [13] A. Srinivas, A. Jabri, P. Abbeel, S. Levine, and C. Finn, "Universal planning networks: Learning generalizable representations for visuomotor control," in *ICML*, 2018.
- [14] X. Chen, Z. Ye, J. Sun, Y. Fan, F. Hu, C. Wang, and C. Lu, "Transferable active grasping and real embodied dataset," in *2020 IEEE International Conference on Robotics and Automation (ICRA)*, 2020, pp. 3611–3618.
- [15] D. Pathak, P. Agrawal, A. A. Efros, and T. Darrell, "Curiosity-driven exploration by self-supervised prediction," in *ICML*, 2017.
- [16] J. Qiu, L. Chen, X. Gu, F. P.-W. Lo, Y.-Y. Tsai, J. Sun, J. Liu, and B. Lo, "Egocentric human trajectory forecasting with a wearable camera and multi-modal fusion," *arXiv:2111.00993*, 2021.
- [17] B. Pan, J. Sun, H. Y. T. Leung, A. Andonian, and B. Zhou, "Cross-view semantic segmentation for sensing surroundings," *IEEE Robotics and Automation Letters*, vol. 5, no. 3, pp. 4867–4873, 2020.
- [18] K. Ehsani, H. Bagherinezhad, J. Redmon, R. Mottaghi, and A. Farhadi, "Who let the dogs out? modeling dog behavior from visual data," in *CVPR*, 2018, pp. 4051–4060.
- [19] J. Bi, J. Luo, and C. Xu, "Procedure planning in instructional videos via contextual modeling and model-based policy learning," in *ICCV*, 2021, pp. 15 611–15 620.
- [20] L. Zhou, C. Xu, and J. Corso, "Towards automatic learning of procedures from web instructional videos," in *AAAI*, 2018.
- [21] D. Zhukov, J.-B. Alayrac, R. G. Cinbis, D. Fouhey, I. Laptev, and J. Sivic, "Cross-task weakly supervised learning from instructional videos," in *CVPR*, 2019, pp. 3537–3545.
- [22] B. Pan, J. Sun, W. Lin, L. Wang, and W. Lin, "Cross-stream selective networks for action recognition," in *2019 IEEE/CVF Conference on Computer Vision and Pattern Recognition Workshops (CVPRW)*, 2019, pp. 454–460.
- [23] D.-A. Huang, L. Fei-Fei, and J. C. Niebles, "Connectionist temporal modeling for weakly supervised action labeling," in *ECCV*, 2016.
- [24] V. Blukis, C. Paxton, D. Fox, A. Garg, and Y. Artzi, "A persistent spatial semantic representation for high-level natural language instruction execution," in *CoRL*, 2021.
- [25] D. Xu, S. Nair, Y. Zhu, J. Gao, A. Garg, L. Fei-Fei, and S. Savarese, "Neural task programming: Learning to generalize across hierarchical tasks," in *ICRA*. IEEE, 2018, pp. 3795–3802.
- [26] D.-A. Huang, S. Nair, D. Xu, Y. Zhu, A. Garg, L. Fei-Fei, S. Savarese, and J. C. Niebles, "Neural task graphs: Generalizing to unseen tasks from a single video demonstration," in *CVPR*, 2019, pp. 8565–8574.
- [27] J.-B. Alayrac, I. Laptev, J. Sivic, and S. Lacoste-Julien, "Joint discovery of object states and manipulation actions," in *ICCV*, 2017.
- [28] W. Yu, W. Chen, S. Yin, S. Easterbrook, and A. Garg, "Modular action concept grounding in semantic video prediction," 2020.
- [29] C. Sun, A. Myers, C. Vondrick, K. Murphy, and C. Schmid, "Videobert: A joint model for video and language representation learning," in *ICCV*, 2019, pp. 7464–7473.
- [30] X. Wang, J.-F. Hu, J.-H. Lai, J. Zhang, and W.-S. Zheng, "Progressive teacher-student learning for early action prediction," in *CVPR*, 2019.
- [31] F. Sener and A. Yao, "Zero-shot anticipation for instructional activities," in *ICCV*, 2019.
- [32] Y. Abu Farha and J. Gall, "Uncertainty-aware anticipation of activities," in *ICCV Workshops*, 2019.
- [33] E. Cohen and C. Beck, "Empirical analysis of beam search performance degradation in neural sequence models," in *ICML*, 2019, pp. 1290–1299.
- [34] C. Meister, T. Vieira, and R. Cotterell, "Best-first beam search," *ACL*, pp. 795–809, 2020.

- [35] D. P. Kingma and J. Ba, “Adam: A method for stochastic optimization,” *ICLR*, 2015.
- [36] J. Carreira and A. Zisserman, “Quo vadis, action recognition? a new model and the kinetics dataset,” in *CVPR*, 2017.
- [37] K. He, X. Zhang, S. Ren, and J. Sun, “Deep residual learning for image recognition,” in *CVPR*, 2016.
- [38] S. Hershey, S. Chaudhuri, D. P. W. Ellis, J. F. Gemmeke, A. Jansen, R. C. Moore, M. Plakal, D. Platt, R. A. Saurous, B. Seybold, M. Slaney, R. J. Weiss, and K. Wilson, “Cnn architectures for large-scale audio classification,” in *ICASSP*, 2017.
- [39] S. Gu, E. Holly, T. Lillicrap, and S. Levine, “Deep reinforcement learning for robotic manipulation with asynchronous off-policy updates,” in *IEEE ICRA*, 2017.